

Photo-oxidation of hydrocarbons in Mexico city effects of altitude. Part I

LUIS G. RUIZ-SUAREZ

Centro de Ciencias de la Atmósfera, Universidad Nacional Autónoma de México, 04510, México, D. F., MEXICO

(Manuscript received on April 15, 1988; accepted in final form August 10, 1988)

RESUMEN

La fotooxidación de n-butano y trans-but-2-eno fue simulada matemáticamente bajo condiciones de irradiación constante (ángulo zenital cero), al nivel del mar y a la altura de la ciudad de México (2234 m). El objetivo fue aproximarse por etapas al conocimiento del efecto de cambios en la irradiación y la presión atmosférica en la formación de ozono en una atmósfera contaminada, los efectos individuales y combinados de la irradiación y presión fueron explorados.

ABSTRACT

The photo-oxidation of n-butane and trans-but-2-ene is simulated under conditions of constant irradiation (normal incidence zero zenith angle) at sea level and at the altitude of Mexico City (2234 m). The object is to understand step by step the effect of changes in irradiation and atmospheric pressure on the production of ozone in a contaminated atmosphere, the individual and combined effects of irradiation and pressure were explored.

Introduction

Mexico City and its conurbated area is the largest and more populated of the world as well as the most contaminated, 85% of the photochemical smog production is due to automobile emissions. On this, several facts need to be pointed out beforehand:

- i) The poor combustion conditions due to the high altitude (2234 meters asl) of the city and the large number of start-stops in the habitual traffic jams.
- ii) To date in Mexico there is only one class of petrol which is of low octane (81, leaded).
- iii) The old age of the vehicle stock with poor maintenance worsened by the long recession since 1982 due to the debt crisis.
- iv) There is no compulsory car performance test.

Measures start to be taken, a pollution monitoring network has been in operation for several years (O_3 , NO_x , SO_2 , CO, Total NMHC's and particles), lead has been reduced in petrol, anti-pollution devices have been fitted in part of the public transport fleet, burning of heavy oil has been replaced partially by natural gas in power stations and in alert conditions they switch to higher ratio of natural gas/heavy oil. Pollution control laws have been actualized and soon car performance test will be compulsory, new leaded and unleaded petrols will be produced.

However up to date the author is not aware of detailed studies of NMHC's in the atmosphere of Mexico City nor of modeling studies of its photochemical smog or of the impact of pollution control measures published in the specialized literature. This work attempts to fill part of this lack of information.

Mathematical modeling of photochemical smog for different pollution scenarios is a common practice tool for evaluating pollution control policies or in pollution alert episodes. However it must be questioned if there are in Mexico City features that make it an special case for modeling both in the physical transport process as in the chemistry.

On the physics, Mexico City is in a valley open to the northeast and the northwest, on the surface the prevailing winds blow towards the southwest. The climate is monsoon like, with a long rain season which helps to wash down some of the pollution, and a dry winter with more stratified winds. The dryness reduces the heating of the boundary layer producing deeper and longer thermal inversions, particulate pollution due to industrial activity, eolic erosion and photochemical smog enhances this effect, furthermore the heat island pulls downslope from surrounding mountains the polluted surface air towards downtown specially during nighttime (Jáuregui, 1988).

On the chemistry, which is the scope of this work, several facts are known:

i) Montly averages of ozone from middle 1986 to middle 1987 exceeded the Mexican ozone norm of 0.11 ppm, this corresponds with the introduction of a new petrol with reduced lead (Bravo *et al.*, 1988).

ii) On one of these days, peak concentrations reached 0.23, 0.35 and 4.5 ppm for nitrogen oxides, ozone and total NMHC's measured on top of the Centre for Atmospheric Sciences building in the University Campus which is about 15 km down wind from the centre of the city and with little vehicle activity (Bravo *et al.*, 1988).

iii) Peak UV irradiation is about three times the peak UV of Los Angeles Cal. (Bravo *et al.*, 1988; Lafonte *et al.*, 1977)

Even when there is no information about the detailed NMHC and concentrations for the Mexico City photochemical smog, reasonable assumptions can be made. First it may be expected that the total and relative concentrations of unsaturated HC's are higher than in developed countries. Second, pressure dependence of some elementary steps may change partition ratios among competing reactions. Special interest is placed on the partition between reaction with olefins and with molecular oxygen for the oxygen atoms as the first reaction is usually left out of the chemical mechanisms used for modeling, and on chain terminating reactions.

Photochemical smog is a very complex reactive mixture, to represent it, the usual approach is to simplify the mechanism in different ways. Grouping HC species in classes and lumping reactions is generally used. One uses surrogate species to represent the chemistry of each lumped class (Atkinson *et al.*, 1982). Other use generalized species to represent the chemistry of each lumped class (McRae *et al.*, 1982; MacCraken *et al.*, 1977). Another uses lumped structures where chemical bonds of the different species are pulled together and the reactions occur not in molecules but on the chemical bonds (see Kilus and Whitten mechanism in McRae *et al.*, 1983). A case apart is Dodge's approach, this does not require detailed characterization of the reacting HC's but divides the total NMHC's in 25% propene and 75% butane with a small percentage of aldehydes (see Dodge's mechanism in McRae *et al.*, 1983 and in Jefries *et al.*, 1981)

However on lumping, some features of the mechanism are over simplified or masked, also from partition rates between competing reactions under typical conditions, some reactions are left out of the lumped mechanism. Atkinson *et al.*, 1982 and Dodge do not include oxygen atoms reaction with olefins, whereas the others do. Atkinson *et al.*, 1982 do not include, reactions of peroxy radicals other than with NO_x, whereas the others do in different ways (McRae *et al.*, 1983). The question is which of this approaches is best suited for Mexico City.

At first glance Dodge's mechanism best fits Mexico City limitations, however is the choice of surrogate species, as well as the percentages the best? Does the exclusion of oxygen atoms reactions has any effect under Mexico City conditions? Furthermore it is known that for an identical set of initial conditions the different mechanisms predict widely different ozone profiles (Jeffries *et al.*, 1981; McRae *et al.*, 1983).

The best way of unveiling any possible special effect of Mexico City conditions is to perform simulations with a detailed mechanism. Such procedure was used by McRae *et al.*, (1983) to compare the performance of the different models for the same set of initial conditions against a detailed mechanism. The size of this mechanism grew up to 217 reactions with very small degree of lumping. Even then, oxygen atoms reactions were left out as well as some peroxy radical reactions. Inclusion of oxygen atoms reactions with unsaturated HC's opens a radical chain, also self and crossed reactions of peroxy radicals may be of importance when nitric oxide concentration drops, specially at high $[NMHC]_0/[NO]_0$ as may be expected in Mexico City.

To bypass the limitations imposed by the scarcity of resources, lack of detailed NMHC studies, lack of a smog chamber to validate results, and a small computer. The problem was broken down. First, up to date detailed mechanisms were constructed for selected HC's (to date n-butane, trans but-2-ene and a mixture of both), trans but-2-ene was chosen to be studied first, in order to reduce the number of reactions and species at this stage of the work. Empirical sensitivity analysis was performed to changes in UV irradiation, initial $[HC]_0/[NO]_0$ ratio, and to changes on the values of the pressure dependent rate constants up to Mexico City conditions. The counter species approach was used. In this paper pure paraffin or olefin cases are discussed. Final results should be compared with smog chamber experiments of surrogate mixtures (McRae *et al.*, 1983).

Procedure

The simulations were carried out with a robust and ready to use dedicated chemical kinetics modeling program (FORTRAN 77) based in the first order, variable step Euler method as implemented by Prothero (1976) and kindly provided by Prof. D. J. Waddington of the University of York. The computer used was a Micro VAX II (2 Mb RAM, 20 Mb virtual memory). Running times were about 4000 s real time in batch, the simulated photolysis times were 15000 s. Graphics were produced with FORTRAN 77 developed programs and output through an IBM compatible with a SweetP 100 plotter attached using VT120 emulation.

Detailed mechanisms for the photo-oxidation of n-butane and trans but-2-ene were constructed (Table 1) using data given by Atkinson and Lloyd (1984), and Baulch *et al.* (1984). All simulations were carried out at 298 K, the pressure dependent rate constants were obtained by the Troe approach as given in Baulch *et al.* (1984) at 1000 and 766 mbar. The pressure dependent rate constants for the addition reactions between alkylperoxy radicals and nitric oxide to give alkyl nitrates were obtained using Atkinson *et al.* (1986) Troe's like approach, this procedure was applied only to the main oxidation paths of the HC's.

The photolysis rates of all species were calculated relative to the photolysis of nitrogen dioxide as given for the Atkinson *et al.* (1982) mechanism in table 22 of McRae *et al.* (1983). Photolysis rates of nitrogen dioxide were estimated for zero zenith angle as given in Fig. 1 in Zafonte *et al.* (1977) for 1000 mbar and for 766 mbar, using $0.22 \text{ cal min}^{-1} \text{ cm}^{-2}$ (Bravo *et al.*, 1988) with (Zafonte *et al.*, 1977):

$$k(\text{min}^{-1}) = (0.079/\cos Z + 0.022) \times \text{radiometric UV}(\text{mWcm}^{-2}).$$

Assuming this empirical formula holds for Mexico City.

TABLE 1
Detailed mechanism for the photo-oxidation of
trans but-2-ene and nbutane

Reaction	Rate const	units	ref
Photolytic Reactions			
1,-	$\text{NO}_2 + h\nu + \text{NO} + \text{O}^*(3\text{P})$	$9,22 \times 10^{-3}$ $1,50 \times 10^{-2}$ $2,45 \times 10^{-2}$	f 2 B1
2,-	$\text{HNO}_2 + h\nu + \text{OH}^* + \text{NO}$	$0,17k_1$	f A2
3,-	$\text{NO}_3 + h\nu + \text{NO}_2 + \text{O}^*(3\text{P})$	$15,60k_1$	f A2
4,-	$\text{NO}_3 + h\nu + \text{NO} + \text{O}_2$	$1,90k_1$	f P
5,-	$\text{O}_3 + h\nu + \text{O}_2 + \text{O}^*(3\text{P})$	$6,46 \times 10^{-3}k_1$	f A2
6,-	$\text{O}_3 + h\nu + \text{O}_2 + \text{O}^*(1\text{D})$	$1,28 \times 10^{-3}k_1$	f D
7,-	$\text{CH}_3\text{ONO} + h\nu + \text{CH}_3\text{O}^* + \text{NO}$	$0,22k_1$	f Mc2
8,-	$\text{CH}_2\text{O} + h\nu + \text{HCO}^* + \text{H}^*$	$3,50 \times 10^{-3}k_1$	f A2
9,-	$\text{CH}_2\text{O} + h\nu + \text{CO} + \text{H}_2$	$3,40 \times 10^{-3}$	f A2
10,-	$\text{CH}_3\text{CHO} + h\nu + \text{CH}_3\text{-}^*\text{CO} + \text{H}^*$	$8,40 \times 10^{-4}k_1$	f A2
Reactions of <i>trans</i> -but-2-ene			
11,-	$\text{OH}^* + \text{CH}_3\text{CH}=\text{CHCH}_3 + \text{CH}_3\text{CH}(\text{OH})-\dot{\text{C}}\text{HCH}_3 + \text{C1ALK}$	$2,40 \times 10^{10}$	s A1
12,-	$\text{O}_2 + \text{CH}_3\text{CH}(\text{OH})-\dot{\text{C}}\text{HCH}_3 + \text{CH}_3\text{CH}(\text{OH})-\text{CH}(\text{O}_2^*)\text{CH}_3$	$6,02 \times 10^9$	s A1
13,-	$\text{NO} + \text{CH}_3\text{CH}(\text{OH})-\text{CH}(\text{O}_2^*)\text{CH}_3 + \text{CH}_3\text{CH}(\text{OH})-\text{CH}(\text{O}^*)\text{CH}_3 + \text{NO}_2 + \text{C4NO}$	$4,19 \times 10^9(0,77 \text{ bar})$ $4,14 \times 10^9(1,00 \text{ bar})$	s A4
14,-	$\text{NO} + \text{CH}_3\text{CH}(\text{OH})-\text{CH}(\text{O}_2^*)\text{CH}_3 + \text{CH}_3\text{CH}(\text{OH})-\text{CH}(\text{ONO}_2)\text{CH}_3$	$3,38 \times 10^9(0,77 \text{ bar})$ $3,92 \times 10^9(1,00 \text{ bar})$	s A4
15,-	$\text{CH}_3\text{CH}(\text{OH})-\text{CH}(\dot{\text{O}})\text{CH}_3 + \text{CH}_3\text{CH}(\text{OH})^* + \text{CH}_3\text{CHO}$	$2,00 \times 10^2$	f A1
16,-	$\text{CH}_3\text{CH}(\text{OH})^* + \text{O}_2 + \text{CH}_3\text{CHO} + \text{HO}_2$	$1,20 \times 10^9$	s A1
17,-	$\text{O}^*(3\text{P}) + \text{CH}_3\text{CH}=\text{CHCH}_3 + \text{CH}_3\text{CH}(\dot{\text{O}})-\dot{\text{C}}\text{HCH}_3 + \text{C1O}$	$1,07 \times 10^{10}$	s A1
18,-	$\text{O}^*(3\text{P}) + \text{CH}_3\text{CH}=\text{CHCH}_3 + \text{CH}_3\text{CO}-\dot{\text{C}}\text{HCH}_3 + \text{H}^* + \text{C2O}$	$2,67 \times 10^9$	s A1
19,-	$\text{CH}_3\text{CH}(\dot{\text{O}})-\dot{\text{C}}\text{HCH}_3 + \text{CH}_3\text{CH}-\text{CHCH}_3$	$1,00 \times 10^3$	f
20,-	$\text{CH}_3\text{CH}(\dot{\text{O}})-\dot{\text{C}}\text{HCH}_3 + \text{CH}_3\text{COCH}_2\text{CH}_3$	$1,0 \times 10^3$	s

Table 1 cont.

21.-	$\text{CH}_3\text{CO}-\dot{\text{C}}\text{HCH}_3 + \text{O}_2 \rightarrow \text{CH}_3\text{CO}-\text{CH}(\text{O}_2)\text{CH}_3$	$6,02 \times 10^6$	s	A1
22.-	$\text{CH}_3\text{CO}-\text{CH}(\text{O}_2)\text{CH}_3 + \text{NO} \rightarrow \text{CH}_3\text{CO}-\text{CH}(\text{O})\dot{\text{C}}\text{H}_3 + \text{NO}_2 + \text{CSNO}$	$4,63 \times 10^9$	s	A1
23.-	$\text{CH}_3\text{CO}-\text{CH}(\text{O})\dot{\text{C}}\text{H}_3 \rightarrow \text{CH}_3-\dot{\text{C}}\text{O} + \text{CH}_3\text{CHO}$	$2,00 \times 10^2$	f	B2
24.-	$\text{O}_3 + \text{CH}_3\text{CH}=\text{CHCH}_3 \rightarrow \text{CH}_3\text{CH}-\overset{\text{O}}{\text{O}}\text{CHCH}_3 + \text{C4ALK}$	$1,20 \times 10^6$	s	A1
25.-	$\text{CH}_3\text{CH}-\overset{\text{O}}{\text{O}}\text{CHCH}_3 + [\text{CH}_3\text{CHO}_2^*]^* \rightarrow \text{CH}_3\text{CHO}$	$1,23 \times 10^9$	f	A1
26.-	$[\text{CH}_3\text{CHO}_2^*]^* \rightarrow \text{CH}_3\text{CHO}_2^*$	$0,66 \times 10^7$	f	A1
27.-	$[\text{CH}_3\text{CHO}_2^*]^* + \overset{\text{O}}{\text{O}}\text{CH}_3\text{CH} (\text{CH3TR})$	$1,00 \times 10^9$	f	A1
28.-	$\text{CH}_3\text{CHO}_2^* + \text{NO} \rightarrow \text{CH}_3\text{CHO} + \text{NO}_2$	$4,22 \times 10^9$	s	A1
29.-	$\text{CH}_3\text{CHO}_2^* + \text{NO}_2 \rightarrow \text{CH}_3\text{CHO} + \text{NO}_3$	$4,22 \times 10^9$	s	A1
30.-	$\text{CH}_3\text{CHO}_2^* + \text{H}_2\text{O} \rightarrow \text{CH}_3\text{COOH} + \text{H}_2\text{O}$	$2,41 \times 10^9$	s	A1
31.-	$\text{CH3TR} \rightarrow \text{CH}_4 + \text{CO}_2$	$2,00 \times 10^9$	f	A1
32.-	$\text{CH3TR} + \text{CH}_3^* \rightarrow \text{CO} + \text{OH}^*$	$1,60 \times 10^9$	f	A1
33.-	$\text{CH3TR} + \text{CH}_3^* \rightarrow \text{CO}_2 + \text{H}^*$	$1,60 \times 10^9$	f	A1
34.-	$\text{CH3TR} + \text{HCO}^* \rightarrow \text{CH}_3\text{O}^*$	$0,80 \times 10^9$	f	A1
35.-	$\text{CH3TR} + \text{CH}_3^* \rightarrow \text{CO}_2 + \text{H}^*$	$0,80 \times 10^9$	f	A1
Reactions of nbutane				
36.-	$\text{HO}^* + \text{CH}_3\text{CH}_2\text{CH}_2\text{CH}_3 \rightarrow \text{CH}_3\text{CH}_2\text{CH}_2\dot{\text{C}}\text{H}_2 + \text{H}_2\text{O}$	$0,16 \times 10^7$	s	A1
37.-	$\text{CH}_3\text{CH}_2\text{CH}_2\dot{\text{C}}\text{H}_2 + \text{O}_2 \rightarrow \text{CH}_3\text{CH}_2\text{CH}_2\text{CH}_2\text{O}_2^*$	$4,52 \times 10^9$	s	A1
38.-	$\text{CH}_3\text{CH}_2\text{CH}_2\text{CH}_2\text{O}_2^* + \text{NO} \rightarrow \text{CH}_3\text{CH}_2\text{CH}_2\text{CH}_2\text{O} + \text{NO}_2 + \text{CNO}_2\text{O}$	$4,46 \times 10^9 (0,77 \text{ bar})$ $4,44 \times 10^9 (1,00 \text{ bar})$	s	A4
39.-	$\text{CH}_3\text{CH}_2\text{CH}_2\text{CH}_2\text{O}_2^* + \text{NO} \rightarrow \text{CH}_3\text{CH}_2\text{CH}_2\text{CH}_2\text{ONO}_2$	$1,24 \times 10^9 (0,77 \text{ bar})$ $1,45 \times 10^9 (1,00 \text{ bar})$	s	A4
40.-	$\text{CH}_3\text{CH}_2\text{CH}_2\text{CH}_2\text{O} + \text{O}_2 \rightarrow \text{CH}_3\text{CH}_2\text{CH}_2\text{CHO} + \text{HO}_2^*$	$4,22 \times 10^9$	s	A1
41.-	$\text{CH}_3\text{CH}_2\text{CH}_2\text{CH}_2\text{O} + \text{CH}_2\text{CH}_2\text{CH}_2\text{CH}_2\text{OH}$	$1,00 \times 10^6$	f	A1
42.-	$\text{CH}_2\text{CH}_2\text{CH}_2\text{CH}_2\text{OH} + \text{O}_2 \rightarrow \text{O}_2\text{CH}_2\text{CH}_2\text{CH}_2\text{CH}_2\text{OH}$	$4,52 \times 10^9$	s	A1
43.-	$\text{O}_2\text{CH}_2\text{CH}_2\text{CH}_2\text{CH}_2\text{OH} + \text{NO} \rightarrow \text{NOCH}_2\text{CH}_2\text{CH}_2\text{CH}_2\text{OH} + \text{NO}_2 + \text{CNO}_2\text{I}$	$4,05 \times 10^9$	s	A1
44.-	$\text{O}_2\text{CH}_2\text{CH}_2\text{CH}_2\text{CH}_2\text{OH} + \text{NO} \rightarrow (\text{NO}_2)\text{OCH}_2\text{CH}_2\text{CH}_2\text{CH}_2\text{OH}$	$0,04 \times 10^4$	s	A1
45.-	$\text{OCH}_2\text{CH}_2\text{CH}_2\text{CH}_2\text{OH} + \text{OHCH}_2\text{CH}_2\text{CH}_2\dot{\text{C}}\text{HOH}$	$5,00 \times 10^6$	f	A1
46.-	$\text{OHCH}_2\text{CH}_2\text{CH}_2\dot{\text{C}}\text{HOH} + \text{O}_2 \rightarrow \text{HOCH}_2\text{CH}_2\text{CH}_2\text{CHO} + \text{HO}_2^*$	$6,02 \times 10^9$	s	A1
47.-	$\text{HO}^* + \text{CH}_3\text{CH}_2\text{CH}_2\text{CH}_3 \rightarrow \text{CH}_3\text{CH}_2\dot{\text{C}}\text{HCH}_3 + \text{H}_2\text{O}$	$1,34 \times 10^9$	s	A1
48.-	$\text{CH}_3\text{CH}_2\dot{\text{C}}\text{HCH}_3 + \text{O}_2 \rightarrow \text{CH}_3\text{CH}(\text{O}_2^*)\text{CH}_3$	$1,02 \times 10^{10}$	s	A1

Table 1 cont.

49,-	$\text{CH}_3\text{CH}_2\text{CH}(\text{O}_2^*)\text{CH}_3 + \text{NO} + \text{CH}_3\text{CH}_2\text{CH}(\text{O}^*)\text{CH}_3 + \text{NO}_2 + \text{CNO}_2$	$4,24 \times 10^9 (0,77 \text{ bar})$	s	A4
		$4,19 \times 10^9 (1,00 \text{ bar})$		
50,-	$\text{CH}_3\text{CH}_2\text{CH}(\text{O}_2^*)\text{CH}_3 + \text{NO} + \text{CH}_3\text{CH}_2\text{CH}(\text{ONO}_2)\text{CH}_3$	$3,38 \times 10^9 (0,77 \text{ bar})$	s'	A4
		$3,92 \times 10^9 (1,00 \text{ bar})$		
51,-	$\text{CH}_3\text{CH}_2\text{CH}(\text{O}^*)\text{CH}_3 + \text{CH}_3\text{CHO} + \text{CH}_3\text{CH}_2^*$	$4,70 \times 10^3$	f	A1
52,-	$\text{CH}_3\text{CH}_2^* + \text{O}_2 + \text{CH}_3\text{CH}_2\text{O}_2^*$	$4,52 \times 10^9 (0,77 \text{ bar})$	t	B
		$2,99 \times 10^9 (1,00 \text{ bar})$		
53,-	$\text{CH}_3\text{CH}_2\text{O}_2^* + \text{NO} + \text{CH}_3\text{CH}_2\text{O}^* + \text{NO}_2 + \text{CNO}_2$	$4,13 \times 10^9$	s	A1
54,-	$\text{CH}_3\text{CH}_2\text{O}_2^* + \text{NO} + \text{CH}_3\text{CH}_2\text{ONO}_2$	$0,0,01 \text{ k}\epsilon_3$	s	A1
55,-	$\text{CH}_3\text{CH}_2\text{O}^* + \text{NO} + \text{CH}_3\text{CH}_2\text{ONO}$	$1,08 \times 10^9$	s	A1
56,-	$\text{CH}_3\text{CH}_2\text{O}^* + \text{NO}_2 + \text{CH}_3\text{CH}_2\text{ONO}_2$	$3,01 \times 10^9$	s	A1
57,-	$\text{CH}_3\text{CH}_2\text{O}^* + \text{O}_2 + \text{CH}_3\text{CHO} + \text{HO}_2^*$	$4,82 \times 10^6$	s	A1
Reactions from acetaldehyde				
58,-	$\text{CH}_3\text{CHO} + \text{OH}^* + \text{CH}_3^*\text{CO} + \text{H}_2\text{O}$	$9,93 \times 10^9$	s	B
59,-	$\text{CH}_3\text{CHO} + \text{O}^*(3\text{P}) + \text{CH}_3^*\text{CO} + \text{OH}^*$	$2,59 \times 10^9$	s	A1
60,-	$\text{CH}_3^*\text{CO} + \text{O}_2 + \text{CH}_3\text{CO}_2^*$	$6,02 \times 10^9$	s	A1
61,-	$\text{CH}_3\text{CO}_2^* + \text{NO}_2 + \text{PAN}$	$2,05 \times 10^9$	t	B2
-61,-	$\text{PAN} + \text{CH}_3\text{CO}_2^* + \text{NO}_2$	$4,20 \times 10^{-4}$	f	B2
62,-	$\text{CH}_3\text{CO}_2^* + \text{NO} + \text{CO}_2 + \text{NO}_2 + \text{CH}_3^*$	$4,80 \times 10^9$	s	A1
63,-	$\text{CH}_3^* + \text{O}_2 + \text{CH}_3\text{O}_2^*$	$8,06 \times 10^9 (0,77 \text{ bar})$	t	B
		$8,57 \times 10^9 (1,00 \text{ bar})$		
64,-	$\text{CH}_3\text{O}_2^* + \text{NO} + \text{CH}_3\text{O}^* + \text{NO}_2 + \text{C}_3\text{NO}$	$4,63 \times 10^9$	s	A1
65,-	$\text{CH}_3\text{O}_2^* + \text{NO}_2 + \text{CH}_3\text{O}_2\text{NO}_2$	$3,24 \times 10^9 (0,77 \text{ bar})$	t	B
		$3,52 \times 10^9 (1,00 \text{ bar})$		
-65,-	$\text{CH}_3\text{O}_2\text{NO}_2 + \text{CH}_3\text{O}_2^* + \text{NO}_2$	2,00	f	
66,-	$\text{CH}_3\text{O}^* + \text{O}_2 + \text{CH}_2\text{O} + \text{HO}_2^*$	$8,19 \times 10^6$	s	B
67,-	$\text{CH}_3\text{O}^* + \text{NO}_2 + \text{CH}_3\text{ONO}_2$	$9,99 \times 10^9$	s	A1
Reactions from formaldehyde				
68,-	$\text{CH}_2\text{O} + \text{OH}^* + \text{HCO}^* + \text{H}_2\text{O}$	$6,02 \times 10^9$	s	B
69,-	$\text{CH}_2\text{O} + \text{O}^*(3\text{P}) + \text{HCO}^* + \text{OH}^*$	$9,65 \times 10^7$	s	A1
70,-	$\text{HCO}^* + \text{O}_2 + \text{CO} + \text{HO}_2^*$	$3,37 \times 10^9$	s	B
71,-	$\text{HO}_2^* + \text{CH}_2\text{O} + \text{HOCH}_2\text{OO}^*$	$4,52 \times 10^7$	s	A1
72,-	$\text{HOCH}_2\text{OO}^* + \text{NO} + \text{HOCH}_2\text{O}^* + \text{NO}_2$	$4,22 \times 10^9$	s	A1
73,-	$\text{HOCH}_2\text{O}^* + \text{O}_2 + \text{CHOOH} + \text{HO}_2^*$	$2,11 \times 10^7$	s	A1

Table 1 cont.

74,-	$\text{HOCH}_2\text{OO}^\bullet + \text{NO} + \text{prod1}$	$2,41 \times 10^{10}$	s	A1
	Inorganic reactions			
75,-	$\text{O}^\bullet(3\text{P}) + \text{O}_2 + \text{O}_3$	$6,49 \times 10^6(0,77 \text{ bar})$ $8,45 \times 10^6(1,00 \text{ bar})$	t	B
76,-	$\text{O}^\bullet(3\text{P}) + \text{NO} + \text{NO}_2$	$1,06 \times 10^9(0,77 \text{ bar})$ $1,35 \times 10^9(1,00 \text{ bar})$	t	B
77,-	$\text{O}^\bullet(3\text{P}) + \text{NO}_2 + \text{NO}_3$	$9,33 \times 10^6(0,77 \text{ bar})$ $1,18 \times 10^9(1,00 \text{ bar})$	t	B
78,-	$\text{OH}^\bullet + \text{NO} + \text{HNO}_2$	$2,88 \times 10^9(0,77 \text{ bar})$ $3,31 \times 10^9(1,00 \text{ bar})$	t	B
79,-	$\text{HO}^\bullet + \text{NO}_2 + \text{HNO}_3$	$6,61 \times 10^9(0,77 \text{ bar})$ $7,82 \times 10^9(1,00 \text{ bar})$	t	B
80,-	$\text{HO}_2^\bullet + \text{NO}_2 + \text{H}_2\text{NO}_4$	$7,37 \times 10^6(0,77 \text{ bar})$ $8,75 \times 10^6(1,00 \text{ bar})$	t	B
-80,-	$\text{H}_2\text{NO}_4 + \text{NO}_2 + \text{HO}_2^\bullet$	$3,88 \times 10^{-2}(0,77 \text{ bar})$ $4,44 \times 10^{-2}(1,00 \text{ bar})$	f	B
81,-	$\text{H}^\bullet + \text{O}_2 + \text{HO}_2^\bullet$	$6,48 \times 10^6(0,77 \text{ bar})$ $8,34 \times 10^6(1,00 \text{ bar})$	t	B
82,-	$\text{NO}_2 + \text{NO}_3 + \text{N}_2\text{O}_5$	$8,79 \times 10^6(0,77 \text{ bar})$ $8,91 \times 10^6(1,00 \text{ bar})$	t	B
-82,-	$\text{N}_2\text{O}_5 + \text{NO}_3 + \text{NO}_2$	$6,29 \times 10^{-2}(0,77 \text{ bar})$ $6,37 \times 10^{-2}(1,00 \text{ bar})$	f	B
83,-	$\text{NO} + \text{NO}_3 + \text{NO}_2 + \text{NO}_2$	$12,0 \times 10^9$	s	B
84,-	$\text{NO} + \text{O}_3 + \text{NO}_2 + \text{O}_2$	$1,08 \times 10^7$	s	B
85,-	$\text{HO}_2 + \text{HO}_2 + \text{H}_2\text{O}_2 + \text{O}_2$	$9,94 \times 10^6$	s	B
86,-	$\text{OH}^\bullet + \text{HO}_2 + \text{H}_2 + \text{O}_2$	$6,62 \times 10^{10}$	s	B
87,-	$\text{OH}^\bullet + \text{HNO}_3 + \text{H}_2\text{O} + \text{NO}_3$	$7,83 \times 10^7$	s	B
88,-	$\text{O}^\bullet(3\text{P}) + \text{NO}_2 + \text{O}_2 + \text{NO}$	$5,60 \times 10^9$	s	B
89,-	$\text{OH}^\bullet + \text{H}_2\text{O}_2 + \text{H}_2 + \text{HO}_2$	$6,62 \times 10^{10}$	s	B
90,-	$\text{OH}^\bullet + \text{O}_3 + \text{HO}_2 + \text{O}_2$	$3,99 \times 10^7$	s	B
91,-	$\text{HO}_2^\bullet + \text{O}_3 + \text{OH}^\bullet + \text{O}_2 + \text{O}_2$	$1,13 \times 10^6$	s	B
92,-	$\text{H}^\bullet + \text{O}_3 + \text{OH}^\bullet + \text{O}_2$	$1,68 \times 10^{10}$	s	B
93,-	$\text{OH}^\bullet + \text{CO} + \text{H}^\bullet + \text{CO}_2$	$1,31 \times 10^6$	s	B
94,-	$\text{HO}_2^\bullet + \text{NO} + \text{NO}_2 + \text{OH}^\bullet$	$5,00 \times 10^9$	s	B
95,-	$\text{NO}_2 + \text{O}_3 + \text{NO}_3 + \text{O}_2$	$1,93 \times 10^4$	s	B

Table 1 cont.

Notes

$$f = s^{-1}$$

$$s = dm^3mol^{-1}s^{-1}$$

$t_3 = dm^3mol^{-2}s^{-1}$, Third order rate constants are actually given as second order after applying Troe's formulae (Baulch *et al* 1984)

References

A1 = Atkinson & Lloyd 1984

A2 = Atkinson *et al* 1982, and Table 23 in McRae *et al* 1983

A3 = Atkinson 1986

A4 = Atkinson *et al* 1987

B = Baulch *et al* 1984

B1 = Bravo 1987

B2 = Batt 1986

D = Table 26 in McRae *et al* 1983

MC2 = Table 25 in McRae *et al* 1983

P = Table 28 in McRae *et al* 1983

Z = Zafonte 1977

The set of initial conditions are given in Tables 2 and 3. All initial concentrations were kept constant except the hydrocarbons and oxygen or nitric oxide which were changed as needed for the sensitivity analysis. Oxygen concentration corresponds to the sea level or Mexico City pressures. The simulations were carried out in $mol\ dm^{-3}$ whereas the results were transformed to ppm afterwards as this is a more usual form. On doing this the effects of pressure are increased as concentrations have to be divided by total pressure in the conversion.

TABLE 2

Initial conditions for the simulated photolysis of *n*-butane ^a at 298 K

Condition	Run 1	Run 2	Run 3	Run 4
$k_1 \times 10^3 (s^{-1})$	9.22	9.22	24.50	24.50
Atmospheric				
Pressure (bar)	1.00	0.77	0.77	1.00
$[O_2] \times 10^3$	8.58	6.74	6.74	8.58
$[n\text{-butane}] \times 10^9$	2.19	2.19	2.19	2.19
$[NO] \times 10^9$	2.19	2.19	2.19	2.19
$[NO_2] \times 10^9$	2.46	2.46	2.46	2.46
$[CH_2O] \times 10^9$	1.55	1.55	1.55	1.55
$[H_2O] \times 10^4$	6.33	6.33	6.33	6.33

Notes

a. - All concentrations in $mol\ dm^{-3}$

TABLE 3

Initial conditions for the simulated photolysis of and *trans* but-2-ene^a at 298 K

Condition	Run 5	Run 6	Run 7	Run 8	Run 9	Run 10	Run 11	Run 12	Run 13
$k_1 \times 10^3$ (s ⁻¹)	9.22	9.22	9.22	9.22	9.22	24.50	24.50	24.50	24.50
Atmospheric									
Pressure (bar)	1.00	0.77	0.77	0.77	0.77	0.77	0.77	0.77	0.77
[O ₂] × 10 ³	8.58	6.74	6.74	6.74	6.74	6.74	6.74	6.74	6.74
[<i>trans</i> but-2-ene] × 10 ³	2.19	2.19	3.29	6.57	21.90	2.19	3.29	6.57	21.90
[NO] × 10 ³	2.19	2.19	2.19	2.19	2.19	2.19	2.19	2.19	2.19
[NO ₂] × 10 ³	2.46	2.46	2.46	2.46	2.46	2.46	2.46	2.46	2.46
[CH ₂ O] × 10 ³	1.55	1.55	1.55	1.55	1.55	1.55	1.55	1.55	1.55
[H ₂ O] × 10 ⁴	6.33	6.33	6.33	6.33	6.33	6.33	6.33	6.33	6.33

Condition	Run 14	Run 15	Run 16	Run 17	Run 18
$k_1 \times 10^3$ (s ⁻¹)	15.00	15.00	15.00	15.00	24.50
Atmospheric					
Pressure (bar)	0.77	0.77	0.77	0.77	1.00
[O ₂] × 10 ³	6.74	6.74	6.74	6.74	8.58
[<i>trans</i> but-2-ene] × 10 ³	2.19	10.95	21.90	21.90	2.19
[NO] × 10 ³	2.19	2.19	2.19	3.40	2.19
[NO ₂] × 10 ³	2.46	2.46	2.46	2.46	2.46
[CH ₂ O] × 10 ³	1.55	1.55	1.55	1.55	1.55
[H ₂ O] × 10 ⁴	6.33	6.33	6.33	6.33	6.33

Notes

a,- All concentrations in mol dm⁻³**Results**

The shape of the concentration profiles of the main products and reactants for the photolysis of n-butane at 1000 mbar and sea level UV (low) irradiation which are not shown here for space sake, compare well with those given in Carter *et al.* (1979) when smog chamber effects are not included. Fig. 1 shows concentration profiles of the main reactants and products for the photolysis of n-butane at 766 mbar and Mexico City (high) irradiation (Run 3). The low reactivity of this mixture even for the most reactive set of conditions is evident. Fig. 2 shows the ozone profiles from the runs 1, 2, 3 and 4 for the photo-oxidation of n-butane. The effect of pressure alone is minimal as the difference between run 1 and 2 is due mainly to the change of units from molar to ppm, irradiation alone has a much larger effect (run 3), reduction of pressure enhances that of irradiation (run 4).

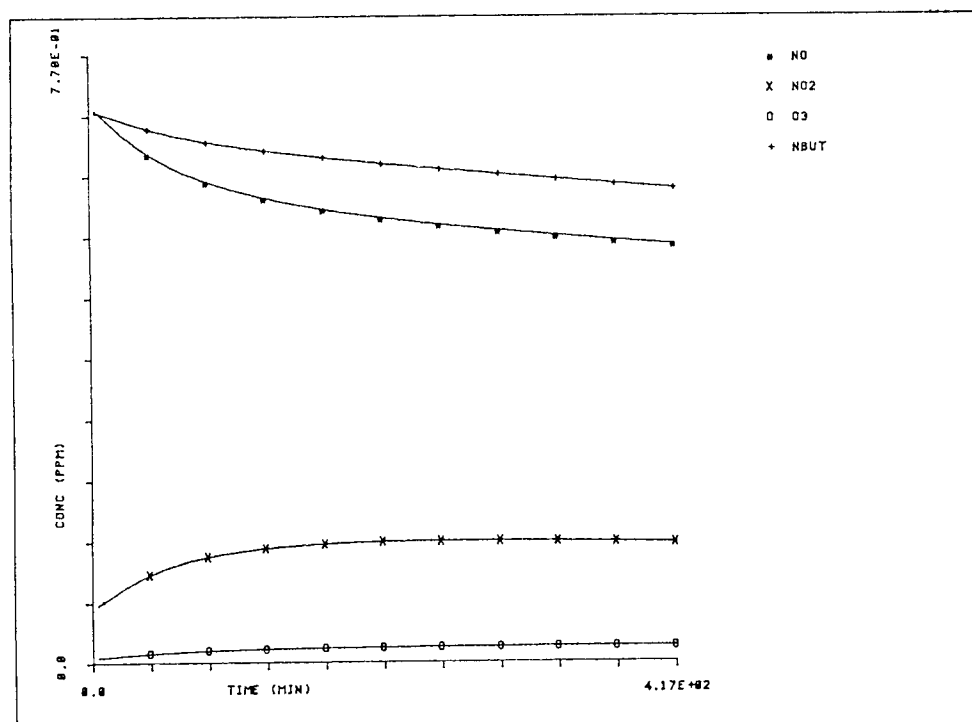


Fig. 1. Photolysis of n-butane (NBUT) at 298 K, 1000 mbar total pressure, Mexico City UV irradiation and $[NBUT]_0/[NO]_0 = 1.0$ (run 3).

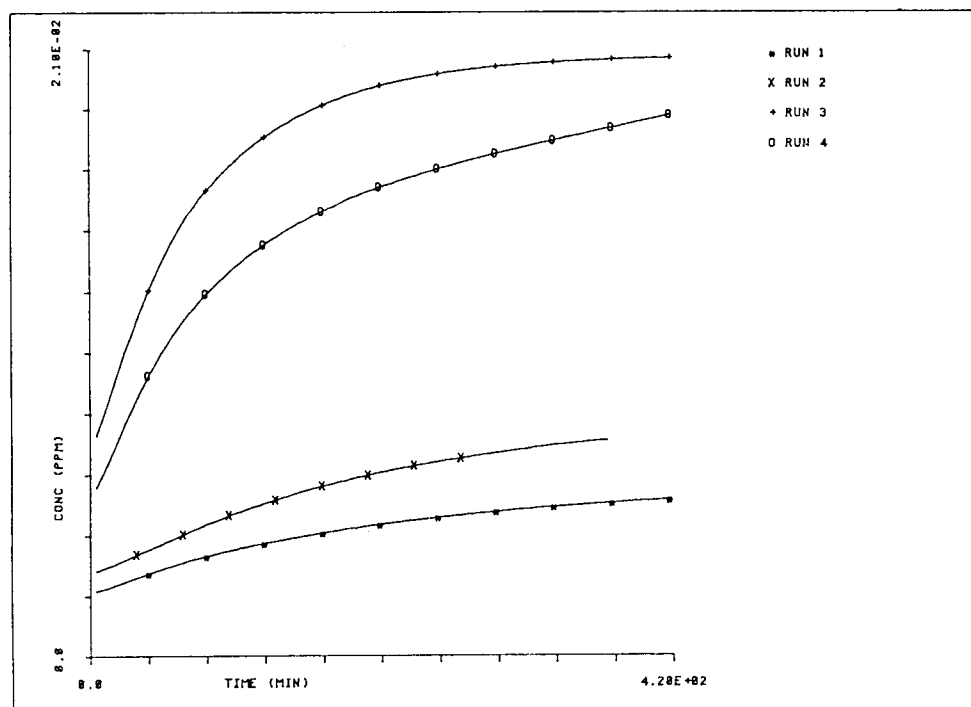


Fig. 2. Ozone concentrations from the photolysis of n-butane at 298 K and under different conditions of pressure and UV irradiation.

Figures 3 and 4 show the concentration profiles of the main products and reactants from runs 5 and 6 for the photo-oxidation of trans-but-2-ene. Initial conditions were the same except that total pressure through molecular oxygen concentration and pressure dependent rate constants were

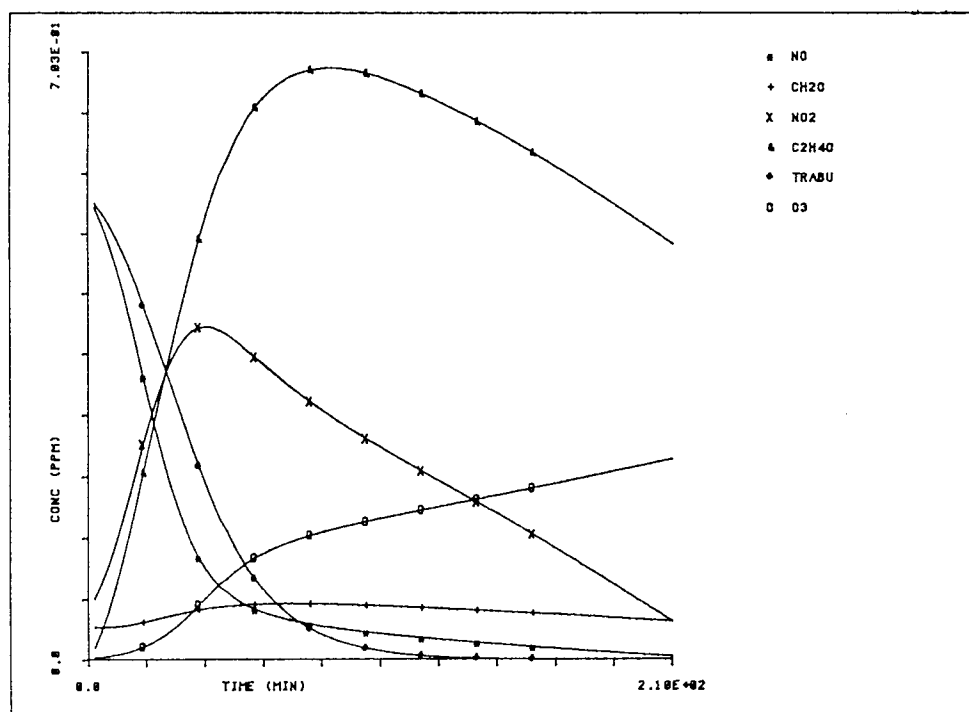


Fig. 3. Photolysis of trans-but-2-ene (TRABU) at 298 K, 1000 mbar total pressure, Los Angeles UV irradiation and $[TRABU]_0/[NO]_0 = 1.0$ (run 5).

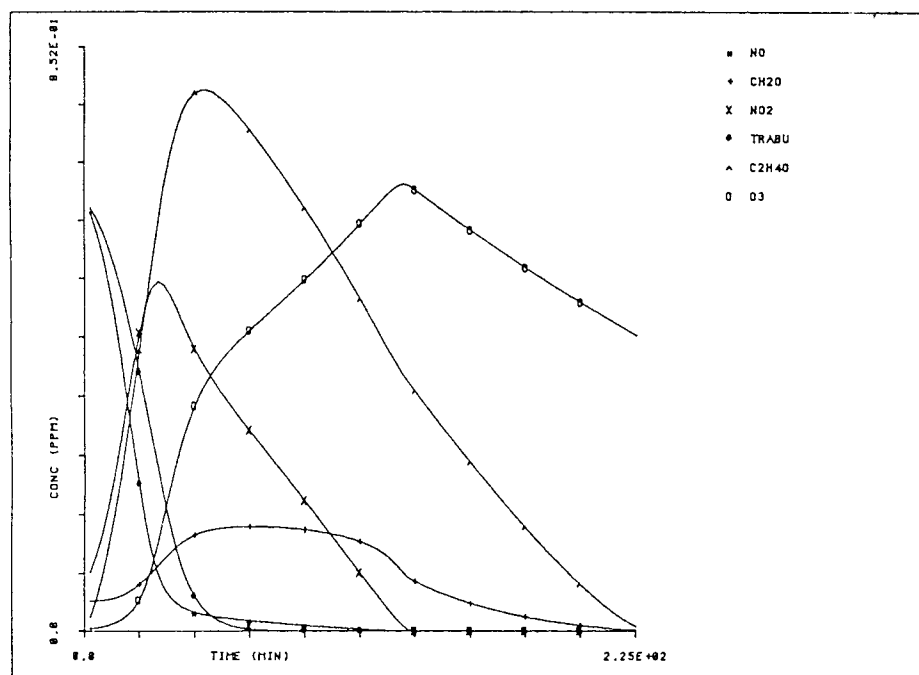


Fig. 4. Photolysis of trans-but-2-ene (TRABU) at 298 K, 766 mbar total pressure, Los Angeles UV irradiation and $[TRABU]_0/[NO]_0 = 1.0$ (run 6).

adjusted with no change in irradiation, the differences are evident. The mixture reacts faster, ozone production is larger. Fig. 5 shows the results from the same set of initial conditions as run 6 with irradiation increased to Mexico City levels (run 8) simulation time is much shorter as the mixture reacts much faster although the shapes are similar, shorter time considered. Fig. 6 shows ozone profiles from runs 5 to 7 and 18, differences due to pressure, irradiation and olefin to nitric oxide ratio, alone or combined are evident.

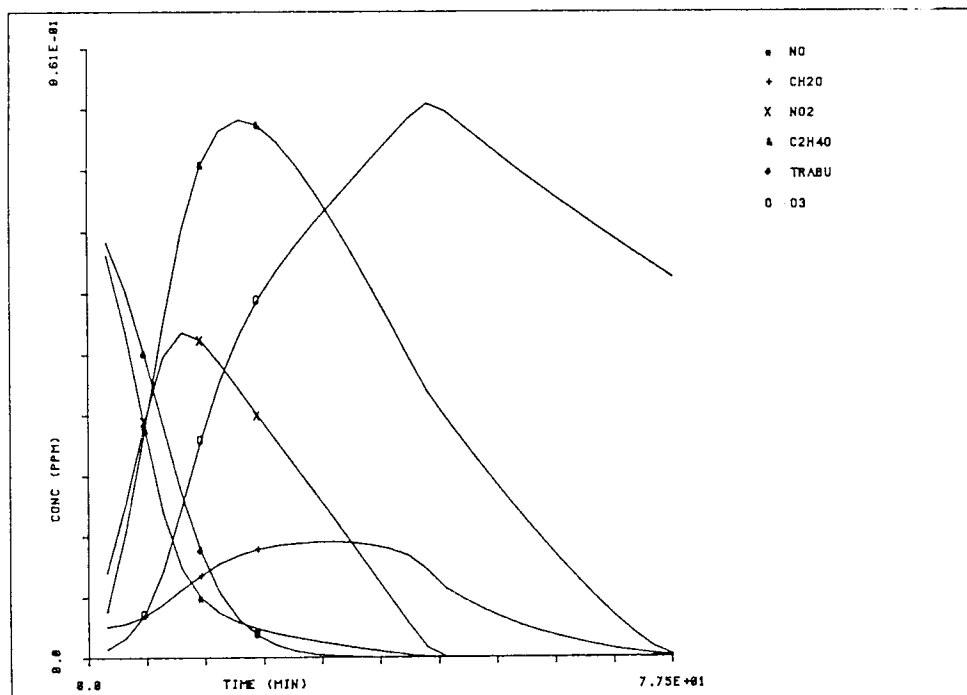


Fig. 5. Photolysis of trans-but-2-ene (TRABU) at 298 K, 766 mbar total pressure, Mexico City UV irradiation and $[TRABU]_0/[NO]_0 = 1.0$ (run 8).

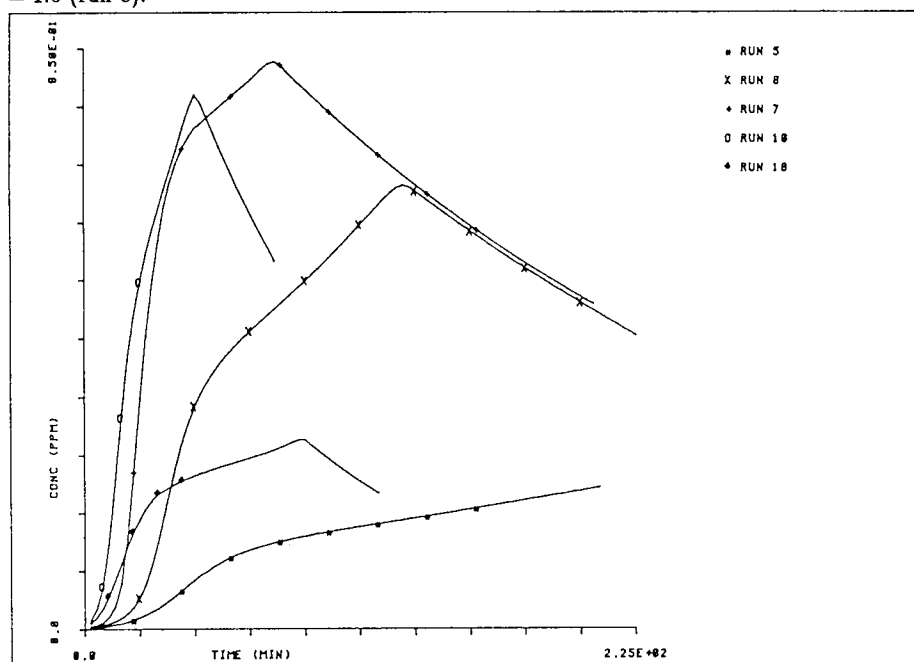


Fig. 6. Ozone concentrations from the photolysis of trans-but-2-ene (TRABU) at 298 K under different conditions of pressure, UV irradiation and $[TRABU]_0/[NO]_0$ ratio.

Discussion

The effect of pressure and irradiation on the photo-oxidation of paraffinic and olefinic hydrocarbons is evident. Paraffinic hydrocarbons are almost insensitive to changes in pressure alone, although the effect of reducing pressure enhances the effect of increased UV intensity.

Trans-but-2-ene is much more sensitive to pressures changes and irradiation, the effect of pressure alone is much larger than for the paraffin. This is mainly due to the primary products formed from both kinds of HC's, for the olefin, almost two liable molecules (acetaldehyde) are formed from each molecule of trans-but-2-ene, whereas for n-butane a wider set of less reactive primary products is formed.

The mechanism by which irradiation and pressure increase overall reactivity in both olefin and paraffin, is by a faster radical input by increased irradiation, and by reducing radical chain terminations such as alkyl nitrate formation and the inorganic addition reactions as nitric acid formation which depend on pressure.

The effect of introducing in the mechanism for the photo-oxidation of trans-but-2-ene the reaction with oxygen atoms (reactions 17 to 23 in Table 1) was investigated at both pressures. At 1000 mbar, the ozone concentration profiles are undistinguishable when the reaction is included or not (off in the figures). At 766 mbar the effect of including it or not depends on total concentrations, olefin to nitric oxide ratio and UV intensity. Keeping initial nitric oxide constant ($2.19 \times 10^{-8} \text{ mol dm}^{-3}$) the difference between the concentrations of ozone simulated with reactions included or not increases with olefin initial concentration (Figs. 7-9) at a ratio of 10:1 for olefin to nitric oxide, the differences depend on UV intensity as follows; at low UV ($k_1 = 0.0092 \text{ s}^{-1}$) the maximum of ozone appears 10 minutes earlier when reactions 17-23 are included but is 7% higher when the reactions are off (Fig. 7). At middle UV intensity ($k_1 = 0.015 \text{ s}^{-1}$) the maximum appears also about 7 minutes earlier but

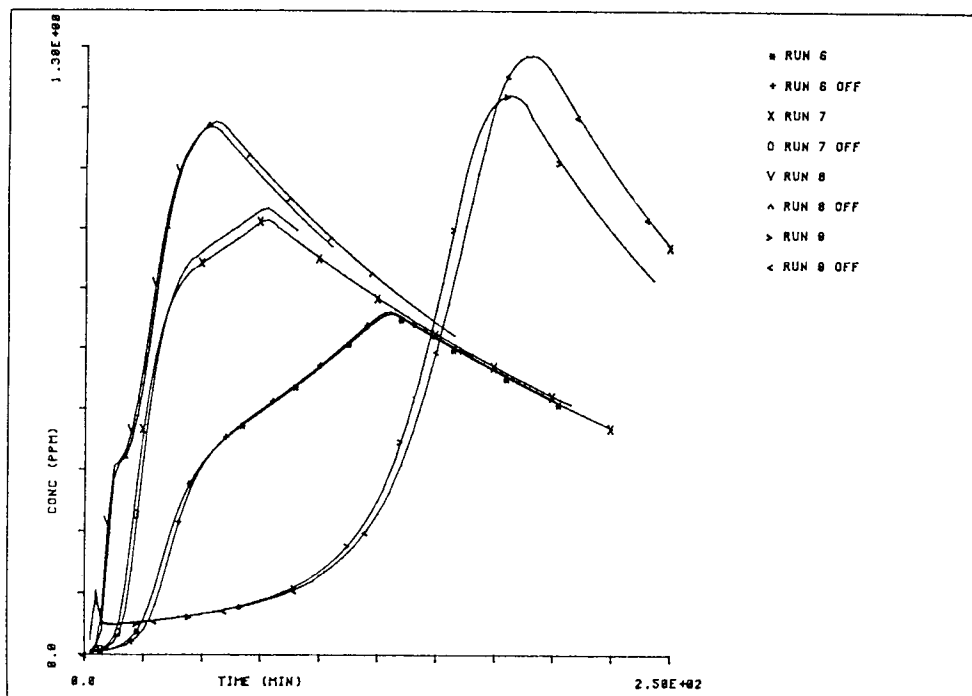


Fig. 7. Comparative effect of neglecting, (off) the addition of oxygen atoms to trans-but-2-ene (TRABU) at low irradiation and different $[TRABU]_0/[NO]_0$ ratio.

now the maximum is higher when the reactions are on (Fig. 8). At the higher UV intensity ($k_1 = 0.0245 \text{ s}^{-1}$) the differences are minimal (Fig. 9). At the middle UV intensity the delays are reduced but the difference between the maxima increases when initial nitric oxide is increased (Fig. 10).

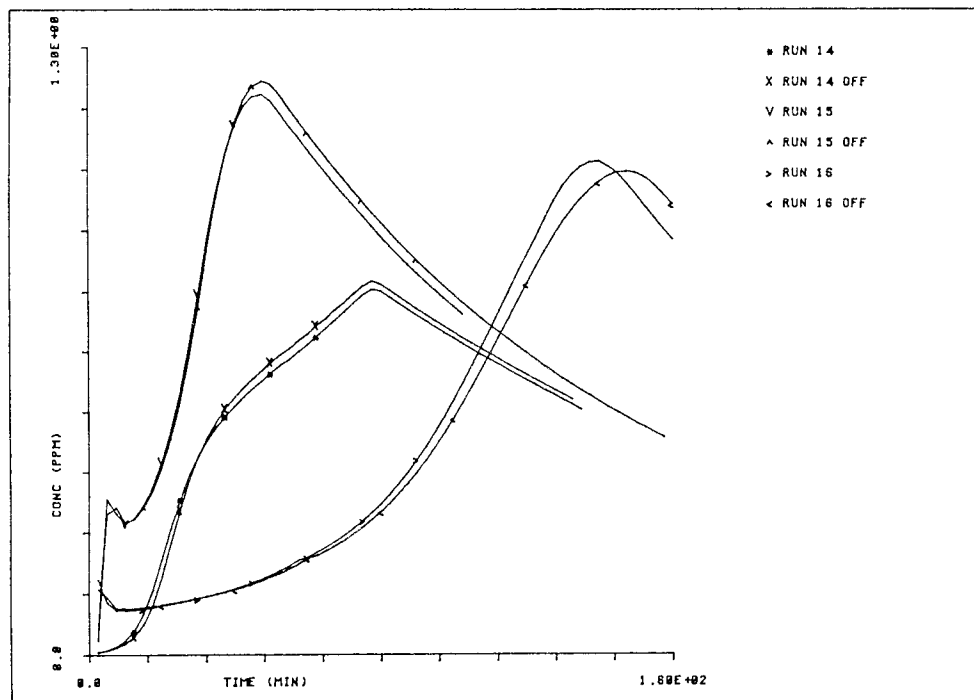


Fig. 8. Comparative effect of neglecting (off) the addition of oxygen atoms to trans-but-2-ene (TRABU) at middle irradiation and different $[TRABU]_0/[NO]_0$ ratio

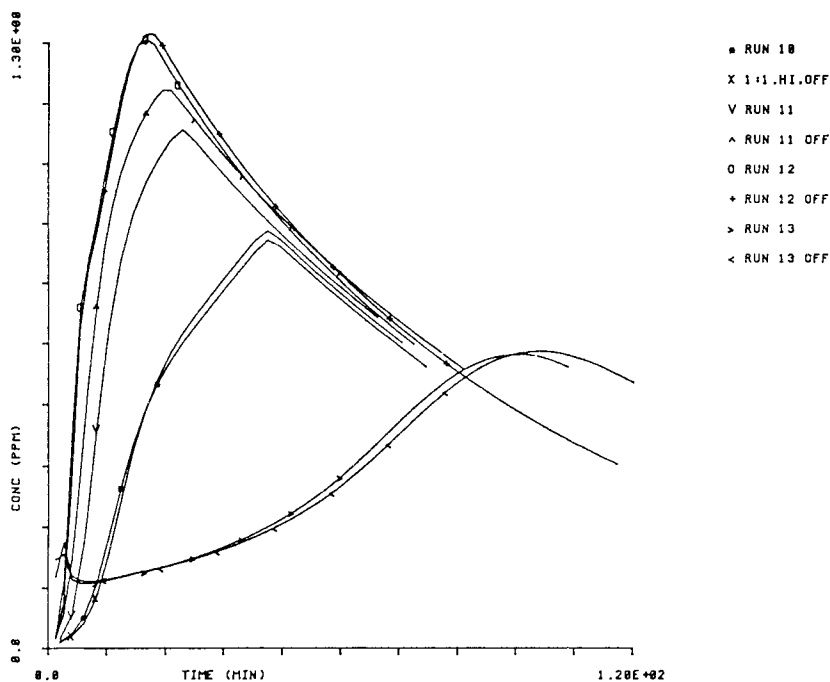


Fig. 9. Comparative effect of neglecting (off) the addition of oxygen atoms to trans-but-2-ene (TRABU) at high irradiation and different $[TRABU]_0/[NO]_0$ ratio.

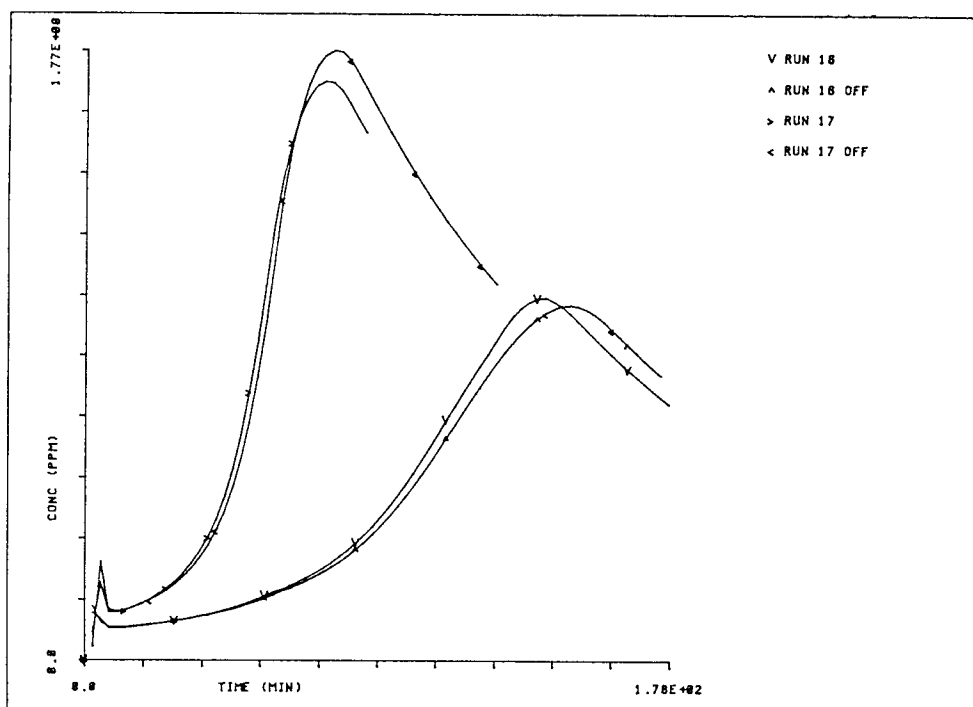


Fig. 10. Comparative effect of neglecting (off) the addition of oxygen atoms to trans-but-2-ene (TRABU) middle and different $[TRABU]_0/[NO]_0$ ratio by increase of $[NO]_0$.

Conclusions

As shown also by other authors (McRae *et al.*, 1983) photochemical rate constants need to be carefully estimated or measured as ozone production rates and concentrations are highly sensitive to them.

It has been shown that an all paraffinic photochemical smog will be almost insensitive to pressure changes alone. Whereas an all olefinic will be highly sensitive to these changes. Increased irradiation enhances the pressure effect for both cases. A real photochemical smog is a complex mixture of paraffins, olefins and aromatic hydrocarbons, the reactivity, potential ozone production rate and ozone maximum at Mexico City conditions (increased irradiation and reduced pressure) compared to that observed at sea level, will depend on the reactivity of the primary and secondary organic pollutants towards chain carriers, as well as to the absolute and relative concentrations of reactive HC's and nitrogen oxides. In this sense, the results obtained here agree with the work by Carter *et al.* (1984) who carried out an experimental sensitivity analysis for the photo-oxidation of a complex HC's mixture (USAF military jet fuel JP-4) and observed that reduced pressure increases nitric oxide oxidation rate.

So far Bravo's *et al.* (1988) are the only set of data found in the literature about HC's in the Mexico City atmosphere. In view of the poor set of data available Dodge's mechanism and total NMHC estimatives seems to be the most wise choice to be used in modeling photochemical smog in Mexico City.

In view of the poor detail of the data on hydrocarbon in Mexico City the exclusion of the addition reaction of oxygen atoms to the olefins does not introduce a significant error in the ozone simulated

concentration profiles at the used and lower concentrations. However at some higher concentrations these reactions may have to be included in the mechanism. Furthermore it should be pointed out that simulations not shown here indicate that the effect of including such reactions is, under certain conditions, similar in magnitude to the effect of considering the pressure dependence of the addition reactions of nitric oxide to alkyl peroxy radicals (i.e., Reaction 14). Therefore the actual relevance of the addition of oxygen atoms to the olefins will depend on their absolute and relative concentrations, irradiation, etc.

As more detailed knowledge of HC's composition becomes available an approach that enables one to make more explicit the pressure dependence of termination reactions such as alkyl nitrate formation will become more useful. Also in Mexico City due to the physical conditions mentioned above, an air parcel is not easily renewed every day, and some stagnation has to be produced. Therefore, further oxidation of the primary products from the photo-oxidation of the initial HC's should have to be included in any chemical mechanism. A mechanism such as Lurman's which is an update and development of Atkinson's *et al.* (1982) and was developed for long range transport will be a better choice.

The author hopes to have shown how sensitive are ozone production rates and ozone maximum to increased irradiation, reduced pressure and the higher HC's and nitrogen oxides emissions occurring in Mexico City. Also how they concatenate to enhance their effects. It is hoped we have shown the urgent need for reliable UV radiometric measurements, reliable correlations between this and photochemical rate constants, or reliable estimates of the latter by absorption and scattering modeling, and of reliable detailed HC's composition studies in Mexico City. Meanwhile, conclusions obtained using current over the counter models will be, to a certain extent, a matter of faith.

Acknowledgements

I wish to thank Prof. D. J. Waddington of the University of York for kindly providing his computer code. To Dr. Carlos Gay for his valuable comments during the development of this work. To M. Sc. Luis Le Moyne, Mr. Rafael Patiño, and personnel of the computer department Inst. of Physic (UNAM) for their help with adapting the program and on developing the FORTRAN graphics subroutines. To Mr. Anastasio López Zavala for useful work.

REFERENCES

- Atkinson, R., A. C. Lloyd and L. Wings, 1982. An updated mechanism for hydrocarbon/ NO_x / SO_2 photo-oxidation suitable for inclusion in atmospheric simulation models. *Atmos. Environ.* **16**, 1341. 1341.
- Atkinson, R., A. C. Lloyd, 1984. Evaluation of Kinetic and Mechanistic Data for Modeling of Photochemical Smog. *J. Phys. Chem. Ref. Data.* **13**, 315.
- Atkinson, R., 1985. Kinetics and mechanism of the gas-phase reactions of the hydroxyl radical with organic compounds under atmospheric conditions, *Chem. Rev.* **85**, 69.
- Atkinson, R., S. M. Aschmann and A. M. Winer, 1987. Alkyl nitrate formation from the reaction of a series of branched RO_2 radicals with NO as a function of temperature and pressure, *J. Atmos. Chem.* **5**, 91.
- Batt, L., 1987. Reactions of alkoxy and alkyl peroxy radicals, *Int. Rev. Phys. Chem.* **6**, 53.

- Baulch, D. L., R. A. Cox, R. F. Hampson Jr., J. A. Kerr, J. Troe and R. T. Watson, 1984. Evaluated kinetic and photochemical data for atmospheric chemistry: suplement II, *J. Phys. Chem. Ref. Data*, **13**, 1258.
- Bravo A., H., F. Perrin G., R. Sosa E. and R. Torres J., 1988. Incremento de la contaminación atmosférica por ozono en la zona metropolitana de la ciudad de México, *Ingeniería Ambiental*, **1**, 8.
- Carter, W. P. L., A. C. Lloyd, J. L. Sprung and J. N. Pitts Jr., 1979. Computer modeling of smog chamber data: progress in validation of a detailed mechanism for the photo-oxidation of propene and n-butane in photochemical smog. *Int. J. Chem. Kinet.*, **11**, 45.
- Carter, W. P. L., R. Atkinson and A. M. Winer, 1984. Effects of temperature and pressure on the photochemical reactivity of a representative aviation fuel. *Environ. Sci. Technol.* **18**, 556.
- Jáuregui, E., 1988. Local wind air pollution interaction in the Mexico basin, *Atmósfera*, **1**, 131.
- Jefries, H. E., K. G. Sexton and C. N. Salmi, 1981. Effects of chemistry and meteorology on ozone control calculations using simple trajectory models and the EKMA procedure. USA Environmental Protection Agency. EPA-450/4-81-024 Research Triangle Park, NC 27711.
- Lurmann, F. W., A. C. Lloyd and R. Atkinson, 1986. A chemical mechanism for use in long-range transport/acid deposition computer modeling. *J. Geophys. Res.*, **91**, 10905.
- MacCracken, M. C., D. J. Wuebbles, J. J. Walton, W. H. Duewer and K. E. Grant, 1977. The Livermore Regional Air Quality Model: I. Concept and Development, *J. Appl. Meteorology*, **17**, 254.
- McRae, G. J., W. Goodin and J. H. Seinfeld, 1982. Development of a second generation mathematical model for urban air pollution I model formulation, *Atmos. Environ.*, **16**, 679.
- McRae, G. J., J. A. Leone and J. H. Seinfeld, 1983. Evaluation of chemical reaction mechanisms for photochemical Smog; USA Environmental Protection Agency, EPA-600/383086, Research Triangle Park NC 27711.
- Prothero, A., 1976. In modern numerical methods for ordinary differential equations. Ed by G. Hall and J. M. Watt. Oxford University Press.
- Zafonte, L., P. L. Reiger and J. R. Holmes, 1977. Nitrogen dioxide photolysis in the Los Angeles atmosphere, *Environ. Sci. & Technol.* **11**, 483.